NASA Technical Memorandum 102865

Dynamic Analysis of Rotor Blade Undergoing Rotor Power Shutdown

Khanh Q. Nguyen

December 1990

National Aeronautics and Space Administration

NASA Technical Memorandum 102865

Dynamic Analysis of Rotor Blade Undergoing Rotor Power Shutdown

Khanh Q. Nguyen, Ames Research Center, Moffett Field, California

December 1990

National Aeronautics and
Space Administration

Ames Research Center
Moffett Field, California 94035-1000

SUMMARY

A rigid flap-lag blade analysis has been developed to simulate a rotor in a wind tunnel undergoing an emergency power shutdown. Results show that for a rotor at a nonzero shaft tilt angle undergoing an emergency power shutdown, the oscillatory lag response is divergent. The mean lag response is large when tested at high collective pitch angles. Reducing the collective pitch during the emergency shutdown reduces the steady lag response. Increasing the rotor shaft tilt angle increases the oscillatory lag response component. The blade lag response obtained by incorporating a nonlinear lag damper model indicates that in this case the equivalent linear viscous damping is lower than originally expected. Simulation results indicate that large oscillatory lag motions can be suppressed if the rotor shaft is returned to the fully vertical position during the emergency power shutdown.

INTRODUCTION

This report describes the rigid-blade analysis of a hovering rotor while it is undergoing an emergency shutdown in rotor power. The results of this report support the safety analysis of the Sikorsky S-76 rotor tested in Ames Research Center's 80- by 120-Foot Wind Tunnel.

During a wind tunnel test of the Sikorsky S-76 rotor, the rotor shaft can tilt as high as 30°. This test condition is necessary to minimize ground effects, and it poses several safety concerns. If an emergency shutdown in rotor power occurs at these critical testing conditions, then the blade lag motions can become large. Large blade lag motions may lead to two drastic consequences: (1) fatigue failure of structural components, and (2) ground resonance. This report analyzes the rotor blade motions subsequent to an emergency shutdown in rotor power.

Ground Resonance – Normal Operating Conditions

Most helicopter rotors tested in a wind tunnel can experience ground resonance. Ground resonance is a violent dynamic instability caused by the coupling between the inplane hub and blade motions, and it occurs only in a certain critical range of the rotor rotational speed. The installation of blade lag dampers is crucial to prevent ground resonance. For this, the damping level is typically sufficient only for the normal operating conditions.

Ground Resonance – Critical Operating Conditions

After an emergency shutdown in rotor power, the rotor speed reduces rapidly. Gravity then becomes a dominant load in the blade aeroelastic responses and can generate large blade lag motions. This is a serious problem, especially for rotors tilted at large shaft angles.

For the Sikorsky S-76 rotor, the lag damper performance is significantly reduced when the blade lag motions exceed a specific value, and if this happens at the critical rotor speed range, then the rotor becomes susceptible to ground resonance.

NOMENCLATURE

A_1	Time constant for rotor speed decay, sec
a	Lift curve slope
a_1	Time constant for dynamic inflow model
c	Blade chord, ft
C_ζ	Equivalent viscous damping coefficient, lb-ft/sec
d_0	Drag coefficient, constant term
d_2	Drag coefficient, quadratic term
e	Hinge offsets for both flap and lag, ft
g	Gravitational constant
I_b	Flapping moment of inertia, slug-ft^2
k_β	Flap hinge spring constant, lb-ft
k_ζ	Lag hinge spring constant, lb-ft
K_β	Pitch-flap coupling (pitch up-flap up is positive)
K_ζ	Pitch-lag coupling (pitch up-lag back is positive)
M_ζ	Lag damper moment, lb-ft
r	Control rate, deg/sec
R	Blade radius, ft
S_b	Blade first moment of inertia, slug-ft
t	Time, sec

v_i	Rotor inflow, ft/sec
x_h	Longitudinal hub displacement (positive aft)
α_s	Rotor shaft tilt angle (positive aft), deg
β	Blade flap (positive up), rad
β_p	Blade precone
ζ	Blade lag (positive aft), rad
ζ_p	Blade pre-lag
Ω	Rotor rotational speed
$\theta_{.75}$	Blade collective pitch at 0.75 blade radius
θ_{1c}	Lateral cyclic pitch
θ_{1s}	Longitudinal cyclic pitch
θ_{tw}	Blade linear pre-twist
σ	Rotor solidity
$\dot{(\ )}$	Time derivative

ANALYTICAL FORMULATION

The analysis is developed for a rotor experiencing a temporal variation in its rotational speed. The rotor blade is modeled as a rigid beam undergoing flap (out-of-plane) and lag (inplane) degrees of freedom. The modeling is valid for rotor blades with linear pre-twist, pre-cone, pre-lag, and kinematic pitch-flap and pitch-lag couplings. Linear quasi-steady aerodynamics is used to represent the blade airloads. Dynamic inflow model based on momentum theory is used to calculate the rotor-induced inflow. The effects of gravity and longitudinal shaft motions are included. Hub flexibility and forward speed effects are not included.

To simulate the rotor power shutdown, the rotor rotational speed is assumed to undergo an exponential decay. The time constant value for the decay rate is taken from the results of the Tunnel Utilization Trainer with Operating Rotor (TUTOR) analysis (ref. 1). This simplification captures the effects of rotor shaft torque dynamics along with motor engine and gearbox dynamics of the drive system for the Ames Rotor Test Apparatus. With this assumption, the rotational speed becomes

$$\Omega(t) = \Omega_o\, e^{-t/A_1} \tag{1}$$

The governing equations for a rigid flap-lag blade are derived by integrating individual components of the blade section moment about the flap and lag hinges. For the Sikorsky S-76 rotor blade, the flap and lag hinges coincide, and therefore the offset value, e, applies for both hinges. These equations are then normalized with respect to I_b, the blade flap moment of inertia. Note that these equations are not normalized with $I_b\Omega^2$ as is the standard practice due to the temporal variation of Ω. The resulting equation for flap is

$$\begin{aligned}
&\ddot{\beta} + \nu_\beta^2\Omega^2\beta + \omega_{\beta 0}^2(\beta - \beta_p) + 2\Omega\beta\dot{\zeta} + g_x\theta_{tw}\sin\Psi - \bar{S}_b(g_x\beta\cos\Psi - g_z - g_x\theta_1\sin\Psi) \\
&+2\dot{\alpha}_s\sin\Psi - \ddot{\alpha}_s\cos\Psi \\
&\quad = \frac{\gamma}{2}\left[(\Omega-\dot{\zeta})^2\left(\frac{\theta_1}{4}+\frac{\theta_{tw}}{5}\right) - (\Omega-\dot{\zeta})\left(\frac{\dot{\beta}-\dot{\alpha}_s\cos\Psi}{4}+\frac{\lambda}{3}\right) + \dot{\alpha}_s\sin\Psi\left(\frac{\lambda}{2}+\frac{\dot{\beta}-\dot{\alpha}_s\cos\Psi}{3}\right)\right. \\
&\quad \left. -\dot{x}_h\sin\Psi(\Omega-\dot{x}_h)\left(\frac{2\theta_1}{3}+\frac{\theta_{tw}}{2}\right) + (\dot{x}_h\sin\Psi)^2\left(\frac{\theta_1}{2}+\frac{\theta_{tw}}{3}\right)\right]
\end{aligned} \tag{2}$$

and that for lag is

$$\begin{aligned}
&\ddot{\zeta} + \nu_\zeta^2\Omega^2\zeta + \omega_{\zeta 0}^2(\zeta-\zeta_p) - 2\Omega\beta\dot{\beta} + \bar{M}\zeta - \dot{\Omega} + (\theta_{tw}+\theta_1\bar{S}_b)(g_x\beta_p\cos\Psi - g_z) \\
&+\bar{S}_b g_x(\sin\Psi - \zeta\cos\Psi) + \bar{S}_b\ddot{x}_h\sin\Psi \\
&\quad = \frac{\gamma}{2}\left[(\Omega-\dot{\zeta})^2\left[\frac{\bar{d}_0}{4}+\bar{d}_2\left(\frac{\theta_1^2}{4}+\frac{2\theta_1\theta_{tw}}{5}+\frac{\theta_{tw}^2}{6}\right)\right]\right. \\
&\quad +(\bar{d}_2-1)\left[\frac{\lambda^2}{2}+\frac{2\lambda(\dot{\beta}-\dot{\alpha}_s\cos\Psi)}{3}+\frac{(\dot{\beta}-\dot{\alpha}_s\cos\Psi)^2}{4}\right] + (1-2\bar{d}_2)(\Omega-\dot{\zeta})\left[\lambda\left(\frac{\theta_1}{3}+\frac{\theta_{tw}}{4}\right)\right. \\
&\quad \left.+(\dot{\beta}-\dot{\alpha}_s\cos\Psi)\left(\frac{\theta_1}{4}+\frac{\theta_{tw}}{5}\right)\right] + \dot{x}_h\sin\Psi\left((1-2\bar{d}_2)\left[-(\dot{\beta}-\dot{\alpha}_s\cos\Psi)\left(\frac{\theta_1}{3}+\frac{\theta_{tw}}{4}\right)\right.\right. \\
&\quad \left.-\lambda\left(\frac{\theta_1}{2}+\frac{\theta_{tw}}{3}\right)\right] + \bar{d}_0\left[\frac{\dot{x}_h\sin\Psi}{2}-\frac{2}{3}(\Omega-\dot{\zeta})\right] + \bar{d}_2\dot{x}_h\sin\Psi\left\{\dot{x}_h\sin\Psi\theta_1\left(\frac{\theta_1}{2}+\frac{2\theta_{tw}}{3}\right)\right. \\
&\quad \left.\left.\left.-\theta_1(\Omega-\dot{\zeta})\left(\frac{2\theta_1}{3}+\theta_{tw}\right)+\theta_{tw}^2\left[\frac{\dot{x}_h\sin\Psi}{4}-\frac{2}{5}(\Omega-\dot{\zeta})\right]\right\}\right)\right]
\end{aligned} \tag{3}$$

where

$$g_x = -\,g\sin\alpha_s/R$$

$$g_y = g\cos\alpha_s/R$$

$$x_h = 0.4745\ \alpha_s \sin\Psi$$

$$\theta_1 = \theta_{.75} + \theta_{1c}\cos\Psi + \theta_{1s}\sin\Psi - 0.75\theta_{tw} + K_\beta\beta + K_\zeta\zeta$$

$$K_\zeta = -0.0125\zeta - 0.00375\beta + 0.00025\beta\theta_{.75} + 0.07875$$

$$\nu_\beta^2 = 1 + \frac{e}{I_b}\int_e^R m(r-e)^2\,dr$$

$$\nu_\zeta^2 = \frac{e}{I_b}\int_e^R m(r-e)^2\,dr$$

$$I_b = \int_e^R m(r-e)^2\,dr$$

$$S_b = \int_e^R m(r-e)\,dr$$

$$\omega_{\beta 0}^2 = k_\beta / I_b$$

$$\omega_{\zeta 0}^2 = k_\zeta / I_b$$

$$\overline{S}_b = R\ \ S_b / I_b$$

$$\overline{d}_0 = d_0 / a$$

$$\overline{d}_2 = d_2 / a$$

$$\lambda = v_i/R$$

$$\Psi = \int_0^t \Omega\,dt$$

Note that the pitch-lag coupling term K_ζ is taken from reference 2 and depends on the blade flap and lag motions as well as the collective pitch angle. The effects of blade flap and lag stops are also included. Due to the lack of information about the stop dynamics, it is assumed that the blade flap or lag motion stops after the blade hits the corresponding stop.

The Sikorsky S-76 rotor employs nonlinear lag dampers. In the present analysis, the effects of both a linear viscous damper model and a nonlinear damper model are studied. For the linear viscous damper,

$$M_\zeta = C_\zeta\,\dot{\zeta}$$

For the nonlinear damper (ref. 3)

$$M\zeta = \begin{cases} 19482\,\dot{\zeta}^2 & \text{for } |5.84\ \dot{\zeta}| < 1 \\ 378 + 454\sqrt{\dot{\zeta}} & \text{for } |5.84\ \dot{\zeta}| > 1 \end{cases}$$

The quantity $5.84\ \dot{\zeta}$ denotes the lag damper velocity in in./sec. From the preceding expression for the nonlinear lag damper model, note that the lag damper performance is drastically reduced when the damper velocity exceeds 1 in./sec. Also let

$$\overline{M}_\zeta = \overline{M}_\zeta / I_b$$
$$\overline{C}_\zeta = \overline{C}_\zeta / I_b$$

The rotor-induced inflow is obtained from momentum theory, and the dynamic effects are included with a first-order time lag. The dynamic inflow equation is

$$\dot{\lambda} = -\frac{1}{a_1}\lambda + \frac{1}{a_1}\sqrt{\frac{C_T}{2}} \tag{4}$$

where

$$C_T = \frac{\sigma a}{2}\left[(\Omega - \dot{\zeta})^2\left(\frac{\theta_1}{3} + \frac{\theta_{tw}}{4}\right) - (\Omega - \dot{\zeta})\left(\frac{\dot{\beta} - \dot{\alpha}_s \cos\Psi}{3} + \frac{\lambda}{2}\right) + (\dot{x}_h \sin\Psi)^2\left(\theta_1 + \frac{\theta_{tw}}{2}\right)\right.$$
$$\left. - \dot{x}_h \sin\Psi(\Omega - \dot{\zeta})\left(\theta_1 + \frac{2\theta_{tw}}{3}\right) + \dot{x}_h \sin\Psi\left(\lambda + \frac{\dot{\beta} - \dot{\alpha}_s \cos\Psi}{2}\right)\right] \tag{5}$$

The value of a_1 is assumed to be 2.0.

Equations (2)-(4) are combined and expressed in a first-order form, and the resulting first-order differential equation is numerically integrated in time using the Gear method (ref. 4).

RESULTS AND DISCUSSIONS

Results are obtained using the properties of the Sikorsky S-76 rotor (ref. 2). The blade and rotor properties used in the simulation are presented in table 1. Figure 1 shows the blade flap and lag frequencies as functions of rotor rotational speed. Due to the matched-stiffness design, the nonrotating flap and lag mode frequencies are equal.

To initiate the time integration, initial conditions have to be prescribed for the rotor degrees of freedom and inflow. For this, a preliminary simulation is performed at a constant rotor speed, and the

initial conditions for the rotor states (blade flap and lag displacements and velocities, and the rotor inflow) are prescribed arbitrarily. The steady state results yield the initial conditions for the actual simulation when the rotor speed decays.

Figure 2 shows the prescribed decay value of the rotor speed as the power is cut off at zero sec, and this rotor speed variation is used in all subsequent simulations.

The first two sets of results represent the shaft-fixed conditions. They are based on the lag damper modeling: (1) linear viscous model, and (2) nonlinear model. The third set of results shows the effects of shaft motions.

Linear Viscous Lag Damper Model

Effect of rotor shaft tilt– Figures 3 and 4 show the effects of shaft tilt on blade responses under a power shutdown condition. The results are presented at three shaft tilt angles: 0, –15, and –30°. The other test parameters and lag damper values are presented in table 2. Figure 3 shows the blade flap responses. Clearly, the blade flaps move downward as rotor speed decreases. After about 30 sec, the blade hits the flap stop at -6° for the three cases shown. Except for the higher harmonics which increase with the higher shaft tilt angle, all the flap responses behave similarly. The higher harmonic flapping motions are due to the Coriolis coupling between the flap and lag motions.

The lag responses are shown in figure 4. The results are presented about the pre-lag angle of 7°. The total blade lag is that shown, as in figure 4 and subsequent figures as well, with an additional 7° of pre-lag. The mean lag (the steady components) is slightly reduced at the higher shaft tilt angles. The oscillatory lag (the higher harmonic components) is moderate at a shaft tilt angle of 15° and increases at a shaft tilt angle of 30°. Note that the oscillatory lag motion is absent at zero shaft tilt angle.

The blade lag response can be considered as a forced response since its general behaviors are dependent on the external forcing. Furthermore, the above results imply that the total lag response can be separated into two components: mean and oscillatory components. These two facts suggest that (1) the rotor speed variations govern primarily the mean lag response behavior, and (2) both the rotor speed variation and the component of gravity acting in the rotor inplane direction govern the oscillatory lag response.

Effect of collective pitch– The effect of collective pitch on blade responses under a power-loss condition are shown next. For these results, four different values of the blade collective pitch are used, ranging from 5 to 18°. The collective pitch remains constant during the power shutdown process. Other parameters used in this simulation are presented in table 2. The blade flap responses shown in figure 5 indicate that different values of collective pitch have different initial blade responses. However, the decay behaviors for these cases are quite similar, and for all four cases shown, the blade hits the flap stop at roughly 30 sec after the power shutdown starts.

Figure 6 shows the lag responses. Even though the steady components of lag response are quite different for different values of collective pitch, they all have a similar oscillatory behavior. When

the blade collective pitch is above 15°, the blade hits the lag stop at 10° (a value measured about a pre-lag angle of 7°) about 32 sec after the power shutdown. From the safety point of view, this is not a major concern since this happens when the rotor speed is low, at about 30 rpm (fig. 2).

Effect of collective pitch reduction rate– In the following simulations, the collective pitch varies during the power shutdown. The control schedule is

$$\theta_{75}(t) = \theta_{75,0} - r*t \tag{6}$$

and $(\theta_{.75})_{min}$ is 2°. In the above expression, r is the control rate, t denotes time in sec, and $\theta_{75,0}$ is the initial collective pitch value. The following set of results is shown in figures 7 and 8 for four different values of r, ranging from 0 to 20 deg/sec. The value of r for the Ames Rotor Test Apparatus is 2 deg/sec. Table 2 presents the values of other parameters used.

The blade flap responses shown in figure 7 indicate that higher values of r result in a shorter decay time. However, the flap responses are essentially the same for the values of r higher than 2.0 deg/sec, except for the short transient behaviors. The similarity in steady state behaviors are expected since the pitch schedule with the higher pitch rate (r > 2 deg/sec) are equal after 5 sec.

For the lag response results shown in figure 8, reducing the collective pitch after a power loss is beneficial because this leads to a smaller steady lag motion and can prevent the blade from hitting the lag stop. The oscillatory components are not affected by the control reduction rate. As in the case with flap response, there is a limiting value to the control rate effectiveness.

Effect of linear viscous damping– The blade responses with different damping values are shown in figures 9 and 10. Other parameters used are also presented in table 2. As shown in figure 9, the flap responses are quite insensitive to the blade lag damper values.

The lag responses shown in figure 10, on the other hand, are quite sensitive to the lag damper values. The steady lag responses decrease slightly, up to 2° maximum, with a larger damping value. The oscillatory lag amplitudes also decrease with an increase in lag damping value.

Nonlinear Lag Damper Model

The study on the effects of rotor shaft tilt and collective pitch on the blade responses under a power shutdown are repeated with the nonlinear lag damper model. The primary test values are shown in table 2. For these results, the flap responses are not shown since, as expected they are found to be similar to those obtained with the linear lag damper model.

Effect of rotor shaft tilt– Figure 11 shows the effects of rotor shaft tilt on the blade lag responses. Even though the general behavior is similar to the results with linear lag damper model (fig. 4), the actual responses are quite different. At zero shaft tilt angle, the lag response still does not exhibit any oscillatory behavior. However, the blade hits the lag stop at 35 sec compared to 42 sec for the same result with the linear lag damper model. At the nonzero shaft tilt angles, the components

of oscillatory lag response are divergent. The oscillatory magnitudes are almost twice those obtained with the linear lag damper model, while the oscillating frequencies remain the same.

Effects of collective pitch– The effect of collective pitch on the blade lag responses with the nonlinear lag damper model are presented in figure 12. Comparing these results to those of figure 6, it is seen that there are two consequences of the nonlinear lag damper model: (1) the blade hits the lag stop earlier, and (2) the oscillatory lag responses are almost twice that of the results shown in figure 6.

Linear vs. Nonlinear Lag Damper Models– The blade lag responses with a linear lag damper model are compared with that with the nonlinear lag damper model in figure 13. For the linear lag damper results, two values of the damping coefficient are used: 2000 and 6000 ft-lb-sec. From figure 13, it can be seen that the lag response using the linear lag damper model with a damping coefficient of 2000 ft-lb-sec is identical to that using the nonlinear lag damper model. This suggests that an equivalent linear viscous damper model with an appropriate damping coefficient can represent a nonlinear damper. The results of figure 13 also indicate that the linear lag damper model with a damping coefficient of 6000 ft-lb-sec is an overestimate of the equivalent viscous damping.

Effects of Rotor Shaft Motions

All the previous results are obtained with the rotor shaft fixed during the emergency power shutdown. For the results of this section, the shaft tilt angle is varied by the expression

$$\alpha_s(t) = \alpha_{s,0} + \dot{\alpha}_s * t \tag{7}$$

where $\alpha_{s,0}$ is the initial shaft tilt angle and $\dot{\alpha}_s$ is the shaft tilt rate. The shaft tilt rate is assumed to be zero once the shaft is brought to the fully upright position, i.e., $\alpha_s = 0°$. The shaft tilt rate for the Ames Rotor Test Apparatus is assumed to be 1 deg/sec. This simulation uses the nonlinear lag damper model, and table 2 presents the values of other parameters used. The flap responses are identical to those of figure 3 and are not shown.

Figure 14 shows the lag responses obtained at different initial shaft tilt angles. The results in this figure show that the oscillatory lag responses are not divergent and are much smaller than those shown in figure 11, corresponding to the nonzero shaft fixed conditions. In fact, the oscillatory lag components all vanish before the blade hits the lag stop. From the safety point of view, these results indicate that large oscillatory lag motions can be avoided if the rotor shaft is returned to the fully vertical position during the emergency power shutdown.

CONCLUSIONS

An analysis based on a rigid flap-lag blade model has been developed and used to predict the aeroelastic responses of a hovering rotor undergoing an emergency shutdown in rotor power. A simulation study is carried out for different rotor properties and operating conditions.

The results indicate that for a rotor tested at a nonzero shaft tilt angle, the oscillatory components of lag response are divergent and can be reduced with an increase in the lag damping. Reducing the collective pitch during the power shutdown reduces the steady component of the lag response. Results with a nonlinear lag damper model suggest that an equivalent linear damper with a damping coefficient of 2000 ft-lb-sec is appropriate to represent the Sikorsky S-76 rotor damper. If the rotor shaft is returned to the fully vertical position during the emergency power shutdown, then the large oscillatory lag motions can be avoided.

REFERENCES

1. Talbot, P. D.; Peterson, R. L.; and Graham, D.: Real-Time Simulation for Helicopter Rotor Wind-Tunnel Operations. Presented at the Computer Simulation Conference, San Diego, CA, Jan. 22-25, 1986.

2. Pace, M.: NASA Ames High Speed Rotor System Design Report, SER51070. Sikorsky Aircraft, Nov. 1987.

3. Kottapalli, S. B. R.: NASA Ames High Speed Rotor System Dynamic Stability Analysis, SER51075. Sikorsky Aircraft, July 1986.

4. IMSL: IMSL Math/Library – Fortran Subroutines for Mathematical Application, Version 1.0., Houston, TX, 1987.

Table 1. Blade and rotor properties used in the simulation model.

$A = 13.16$ sec	$\beta_{max} = 21$ deg
$a = 5.73$	$\beta_{min} = -6$ deg
$a_1 = 2.0$ sec	$\beta_p = 0.0$ deg
$e = 0.833$ ft	$\gamma = 10.09$
$d_0 = 0.0087$	$n_\beta = 1.0296$
$d_2 = 0.1719$	$\nu_\zeta = 0.2470$
$c = 1.29$ ft	$\sigma = 0.0748$
$I_b = 408$ slug-ft^2	$\theta_{tw} = -10$ deg
$k_\beta = 1192$ ft-lb	$\theta_{1c} = 0.00$ deg
$k_\zeta = 1192$ ft-lb	$\theta_{1s} = 0.00$ deg
$K_\beta = -0.305$	$\zeta_{max} = 17$ deg
$R = 22.0$ ft	$\zeta_{min} = -5$ deg
$S_b = 30$ slug-ft	$\zeta_p = 7$ deg

Table 2. Values of test parameters used in the simulations.

Figures	α, deg	θ_{75}, deg	r, deg/sec	C_ζ, ft-lb-sec
3, 4, 11	Varies	10	0.0	6000*
5, 6, 12	-15	Varies	0.0	6000*
7, 8	-15	10	Varies	6000*
9, 10	-15	10	0.0	Varies
13	–15	10	0.0	
14	Varies	10	0.0	

*For linear lag damper model only.

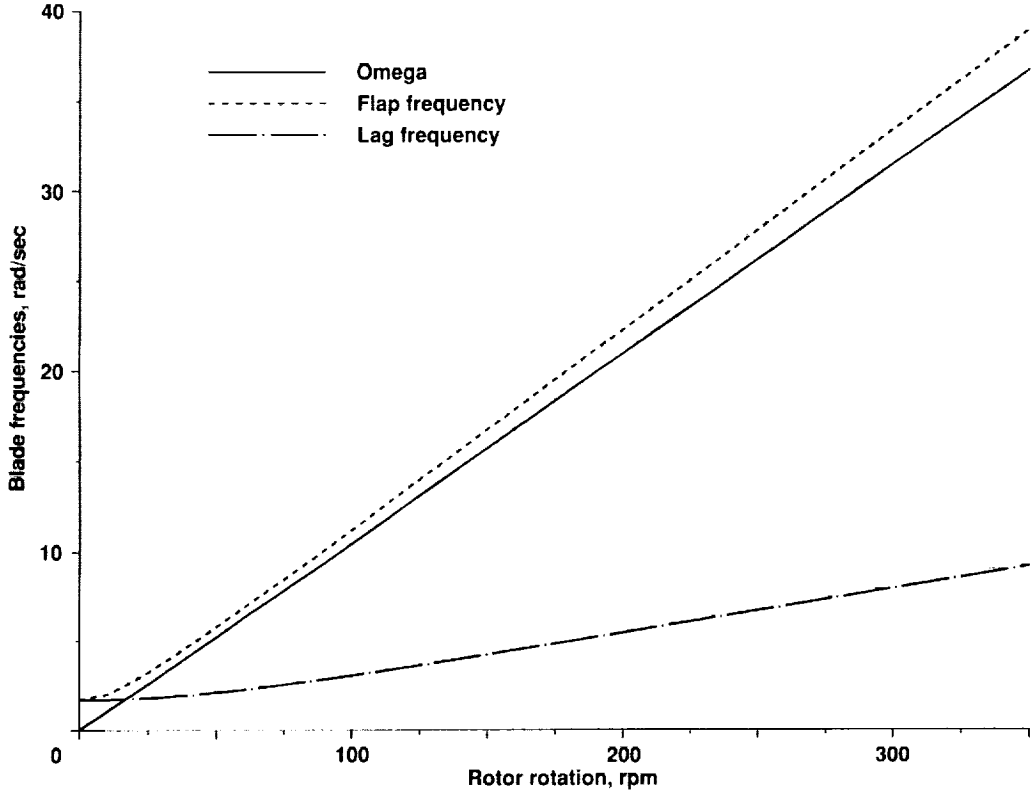

Figure 1. Sikorsky S-76 rotor blade frequencies.

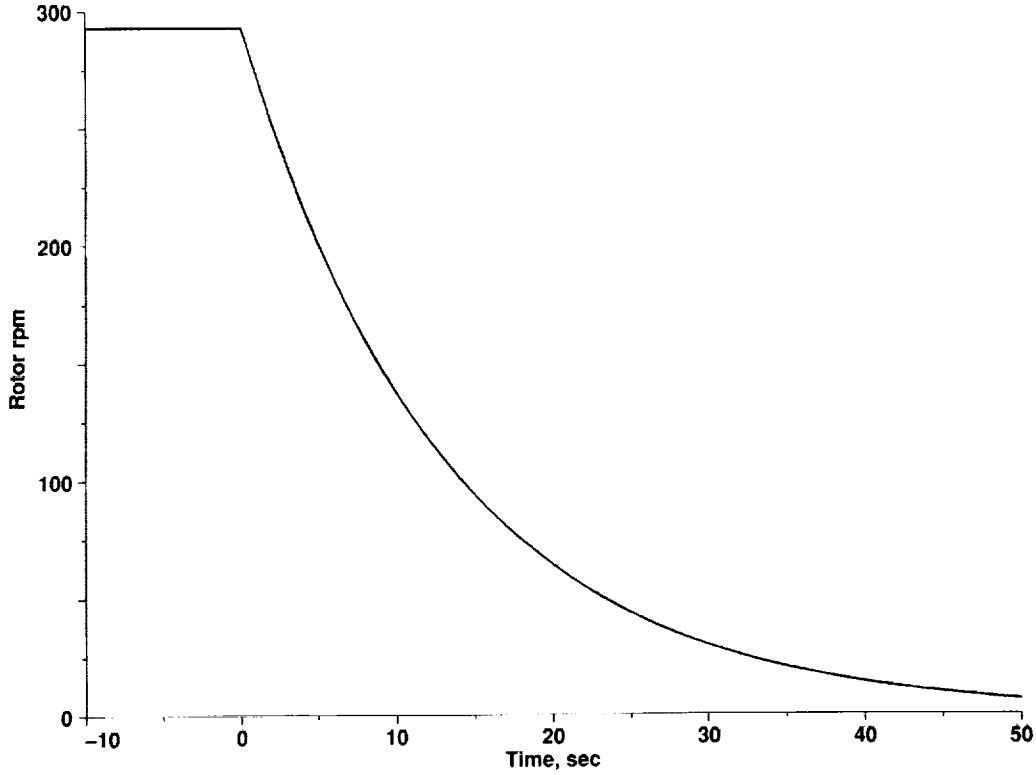

Figure 2. Rotor rpm variation used in the simulation study.

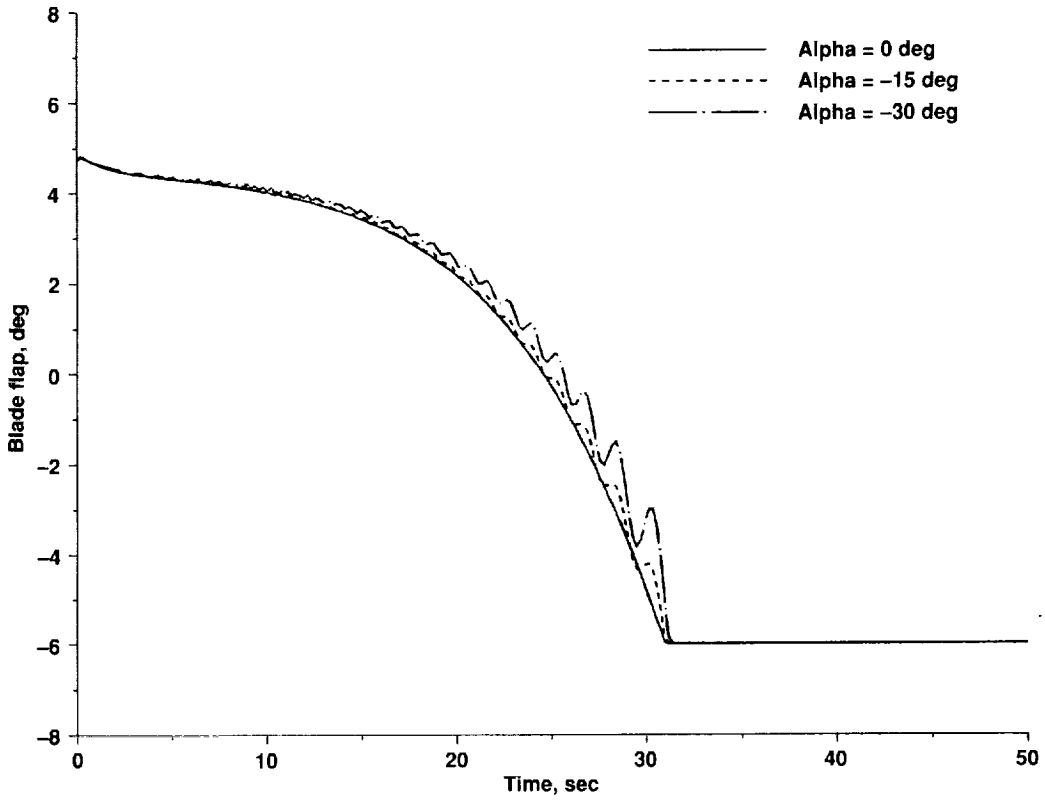

Figure 3. Effects of shaft tilt on flap response of rotor undergoing an emergency shutdown in rotor power.

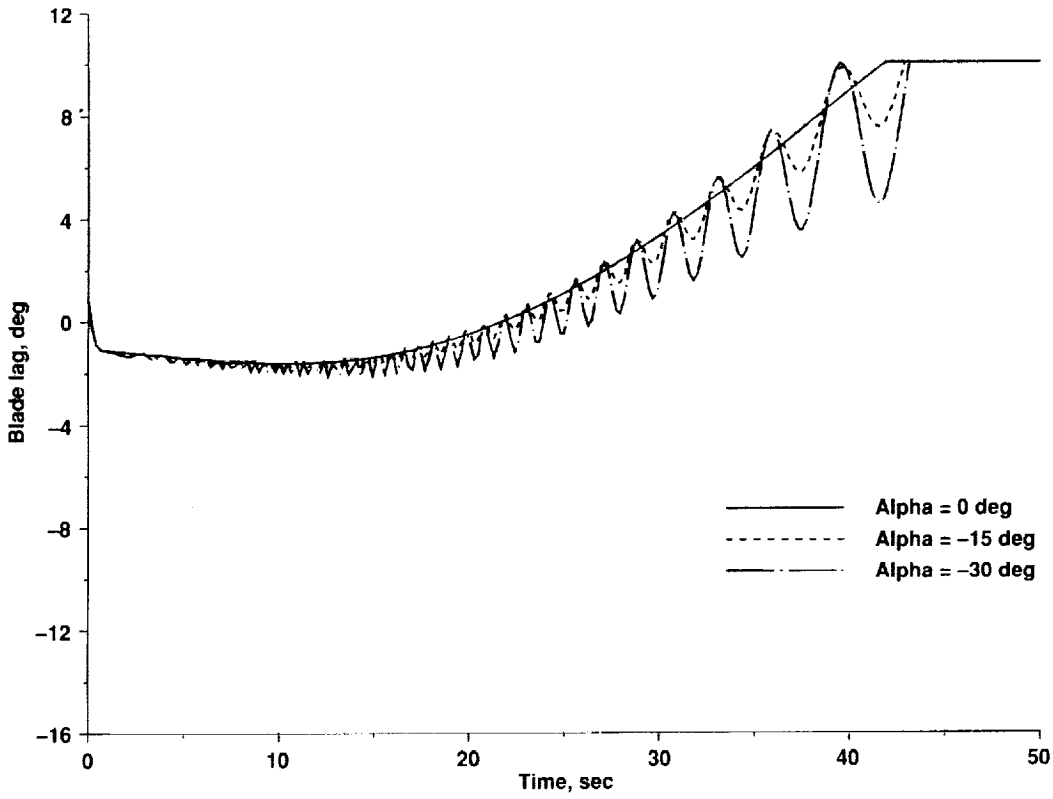

Figure 4. Effects of shaft tilt on lag response of rotor undergoing an emergency shutdown in rotor power.

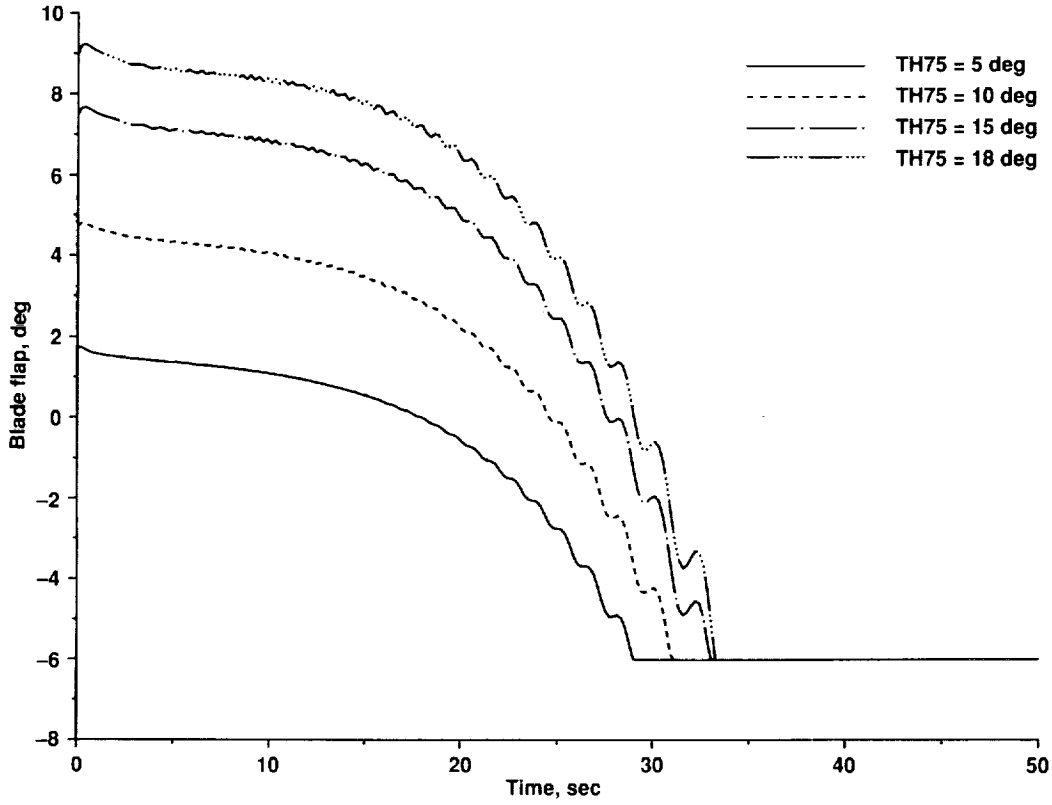

Figure 5. Effects of collective pitch on flap response of rotor undergoing an emergency shutdown in rotor power.

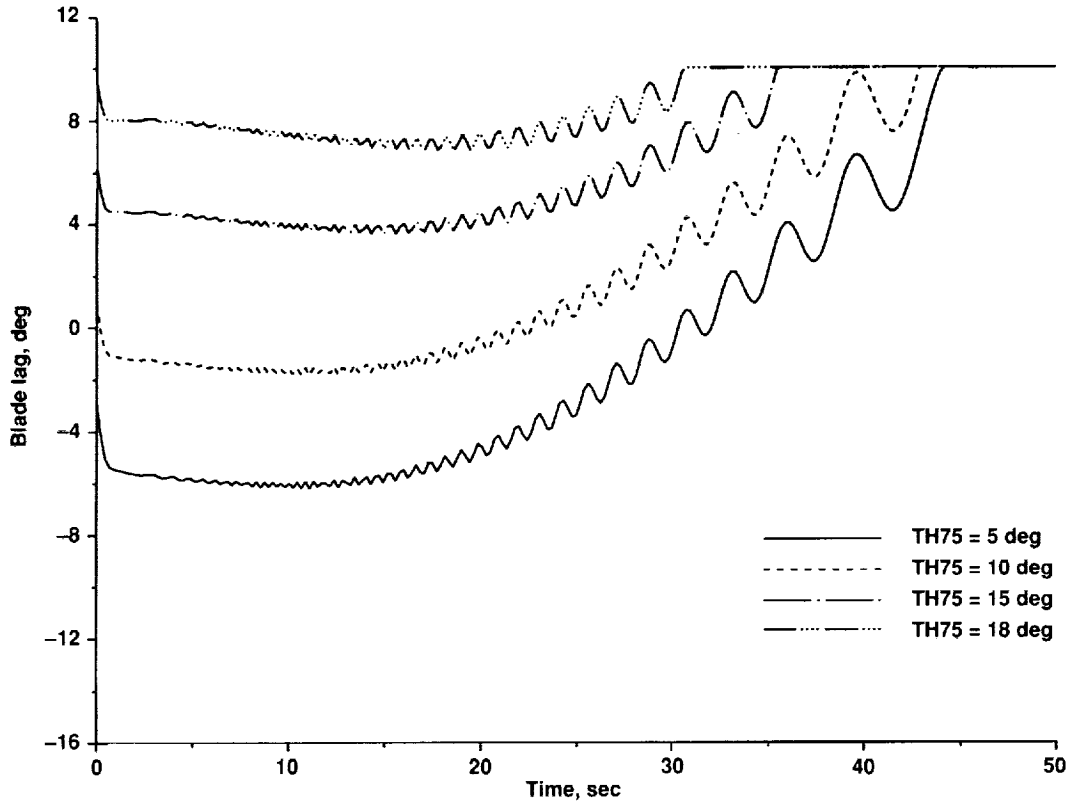

Figure 6. Effects of collective pitch on lag response of rotor undergoing an emergency shutdown in rotor power.

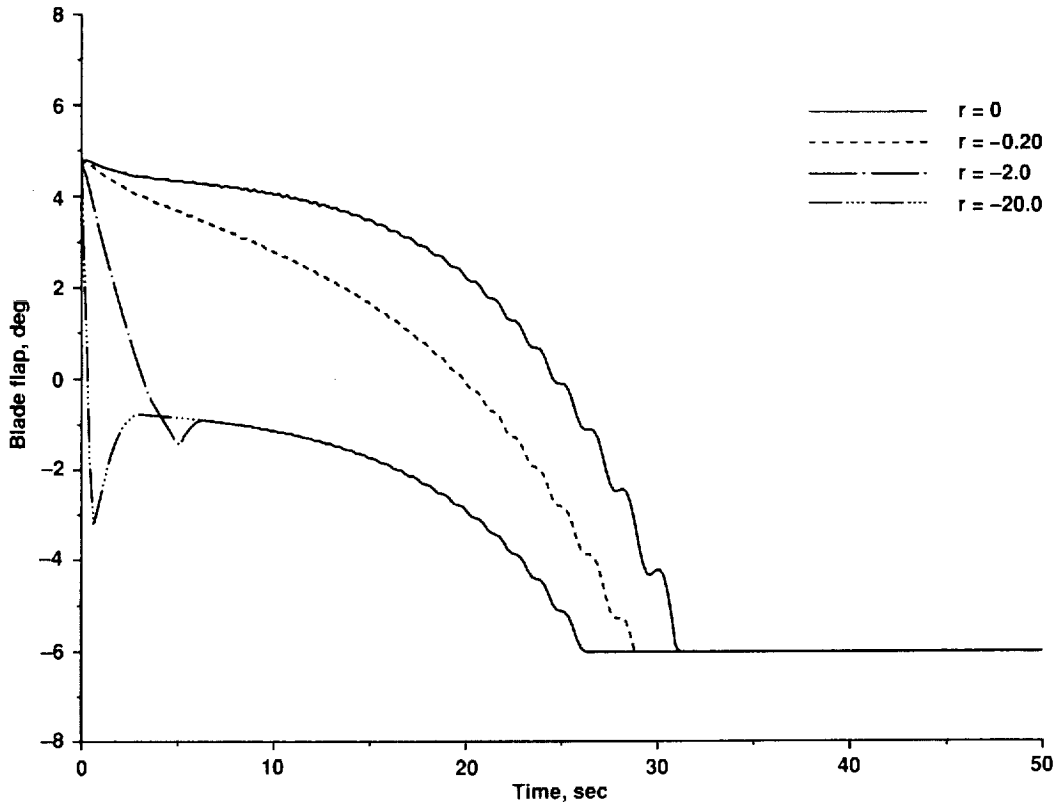

Figure 7. Effects of collective pitch rate on flap response of rotor undergoing an emergency shutdown in rotor power.

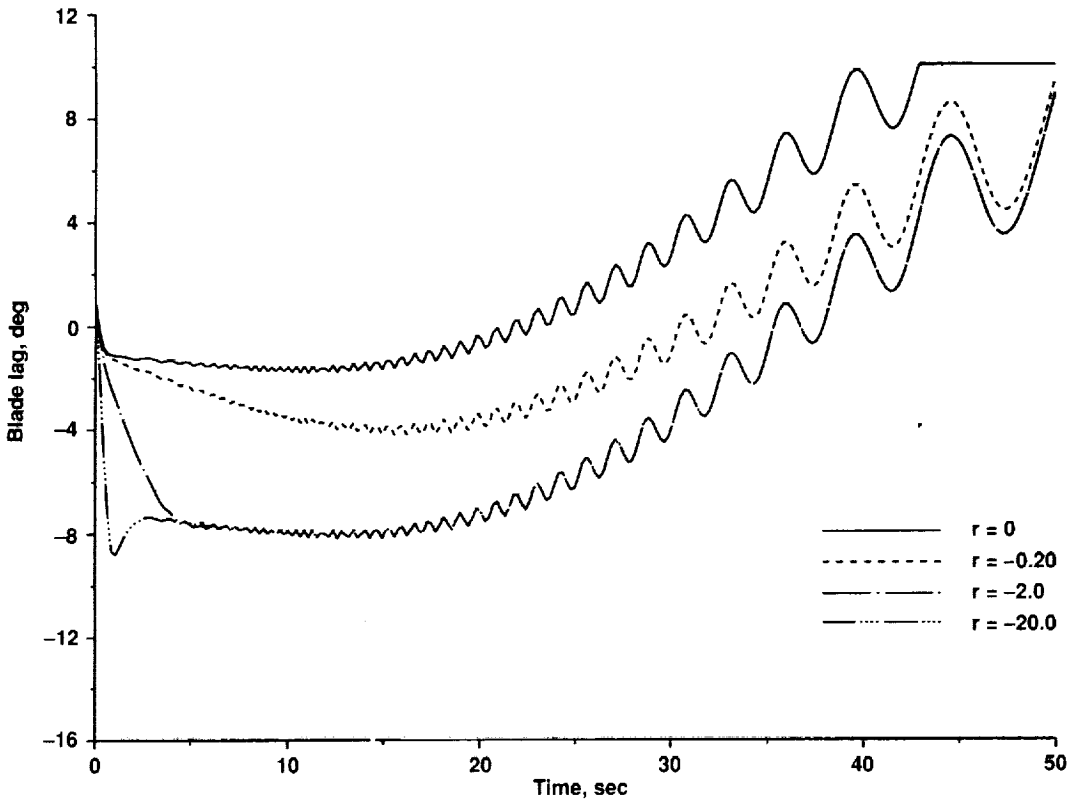

Figure 8. Effects of collective pitch rate on lag response of rotor undergoing an emergency shutdown in rotor power.

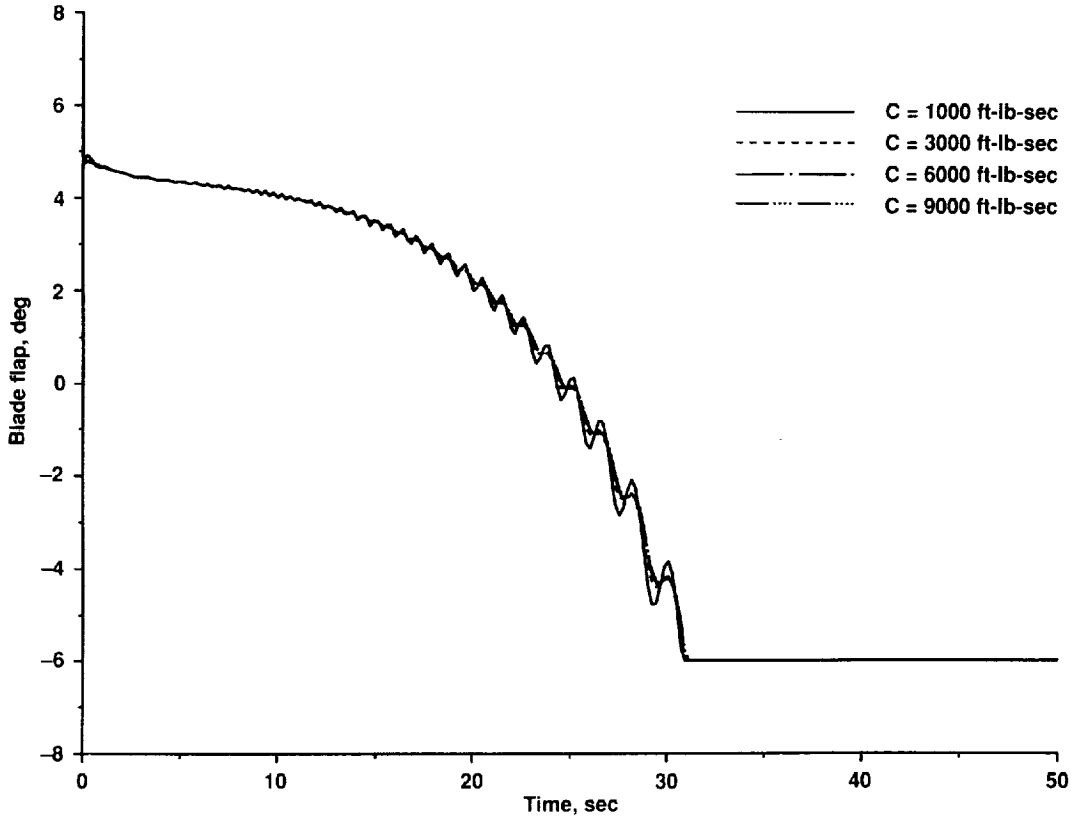

Figure 9. Effects of lag damping amplitude on flap response of rotor undergoing an emergency shutdown in rotor power.

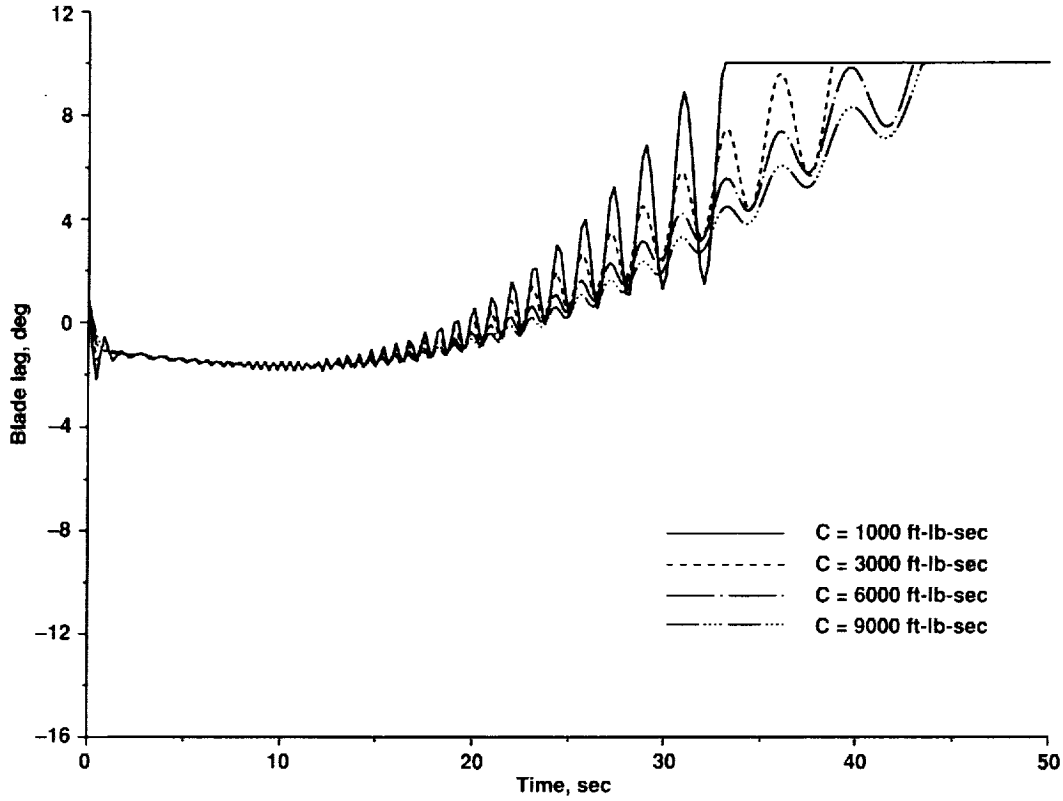

Figure 10. Effects of lag damping amplitude on lag response of rotor undergoing an emergency shutdown in rotor power.

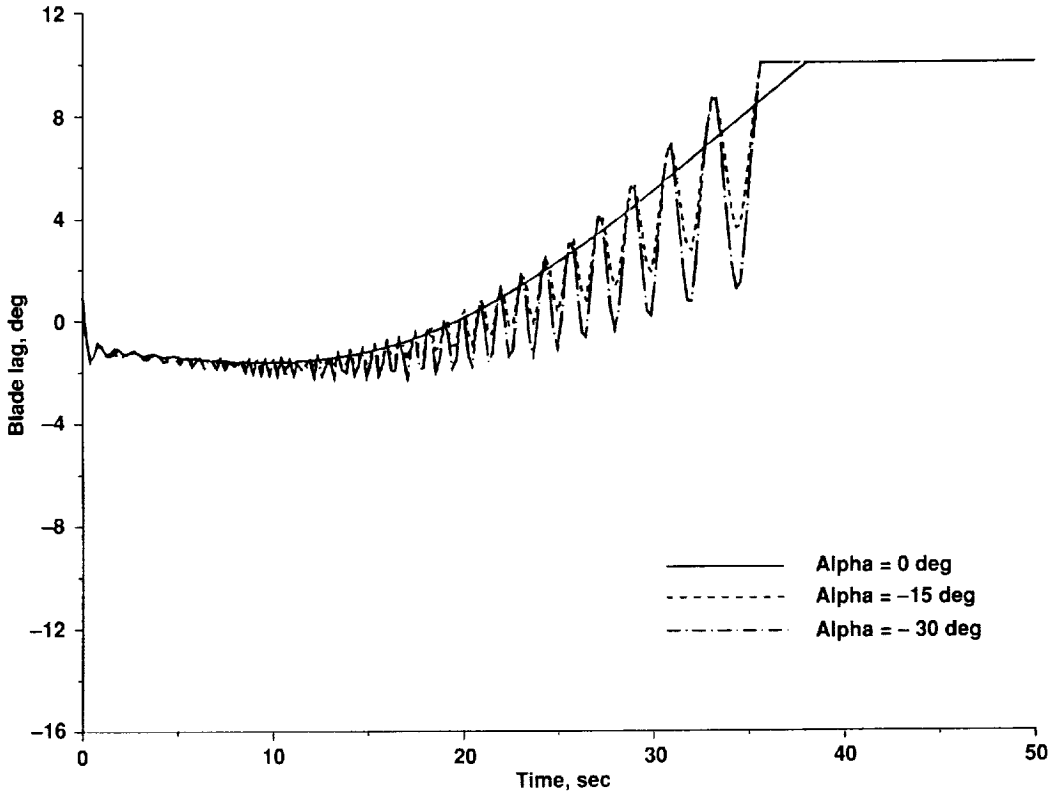

Figure 11. Effects of shaft tilt on lag response of rotor undergoing an emergency shutdown in rotor power–nonlinear lag damper model.

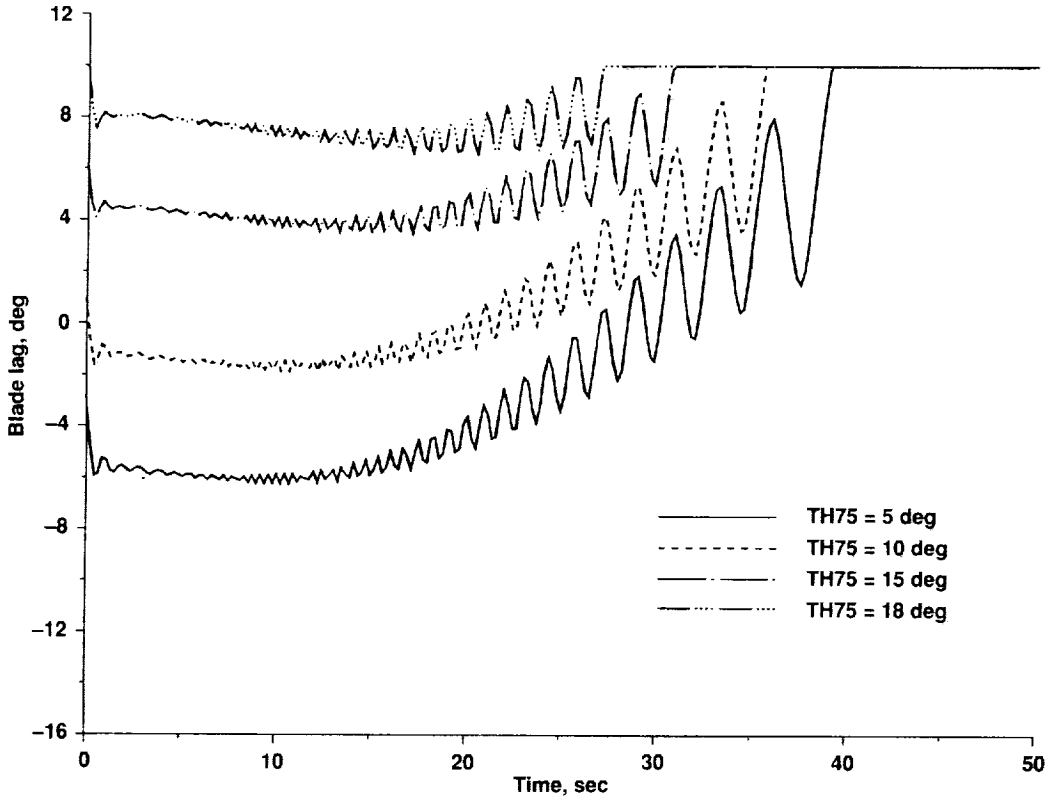

Figure 12. Effects of collective pitch on lag response of rotor undergoing an emergency shutdown in rotor power–nonlinear lag damper model.

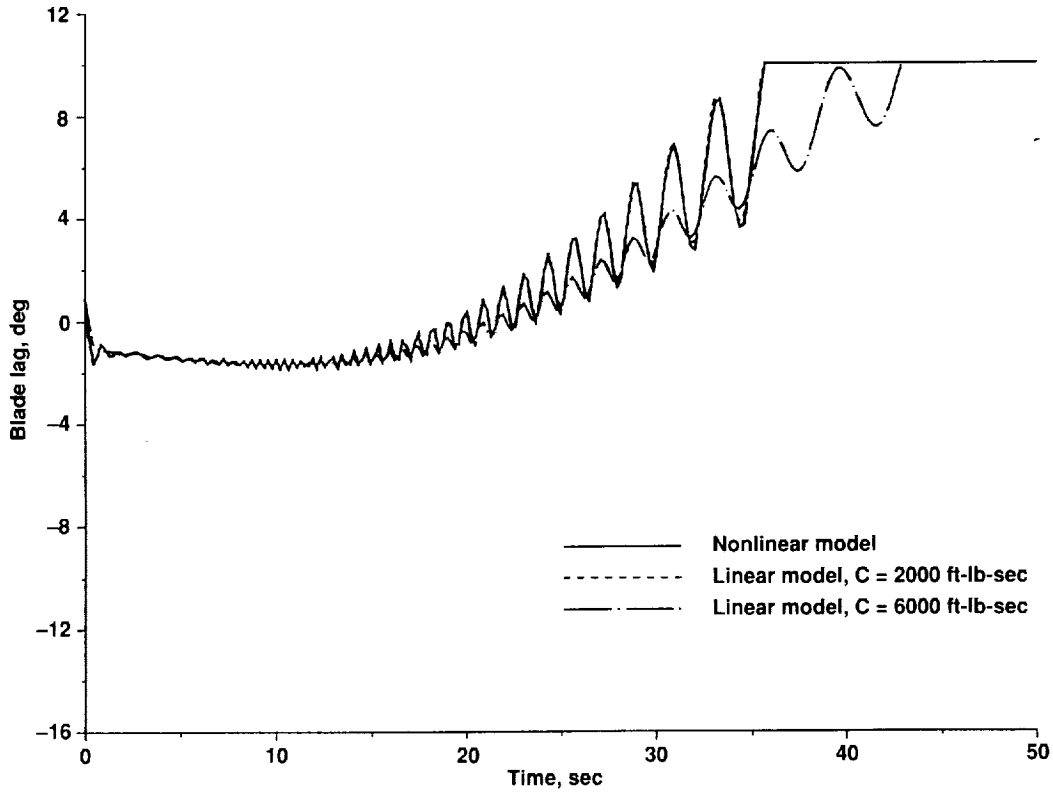

Figure 13. Effects of lag damper model on lag response of rotor undergoing an emergency shutdown in rotor power.

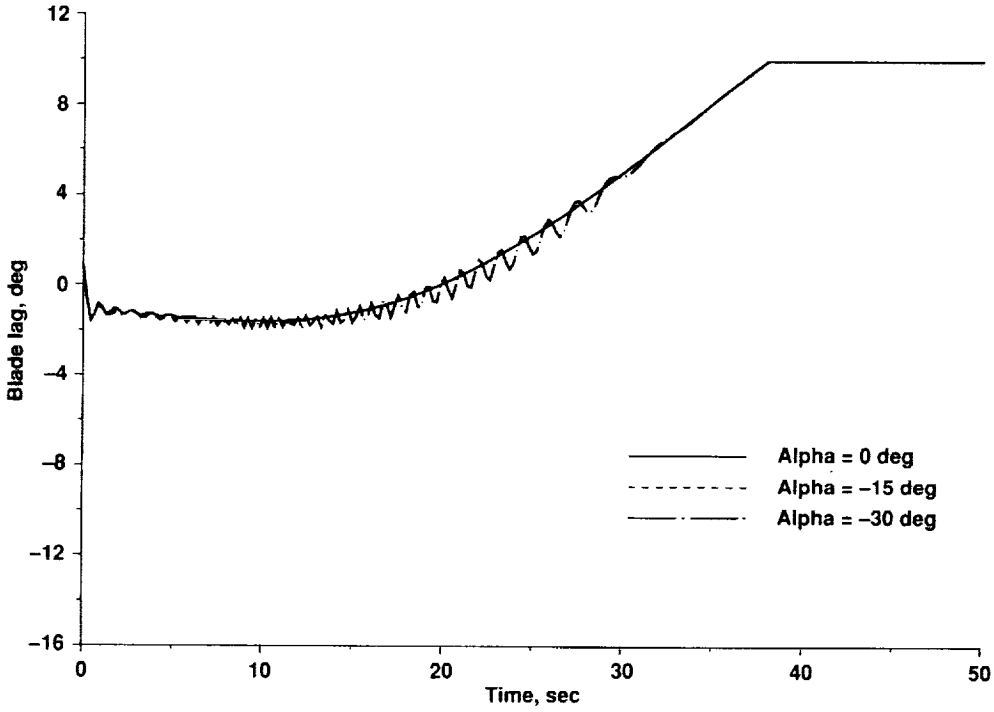

Figure 14. Effects of shaft motion on lag response of rotor undergoing an emergency shutdown in rotor power.

NASA
National Aeronautics and Space Administration

Report Documentation Page

1. Report No.	2. Government Accession No.	3. Recipient's Catalog No.
NASA TM-102865		

4. Title and Subtitle	5. Report Date
Dynamic Analysis of Rotor Blade Undergoing Rotor Power Shutdown	December 1990
	6. Performing Organization Code

7. Author(s)	8. Performing Organization Report No.
Khanh Q. Nguyen	A-90284
	10. Work Unit No. 505-61-51

9. Performing Organization Name and Address	11. Contract or Grant No.
Ames Research Center Moffett Field, CA 94035-1000	
	13. Type of Report and Period Covered Technical Memorandum

12. Sponsoring Agency Name and Address	14. Sponsoring Agency Code
National Aeronautics and Space Administration Washington, DC 20546-0001	

15. Supplementary Notes

Point of Contact: Khanh Nguyen, Ames Research Center, MS T-042, Moffett Field, CA 94035-1000
(415) 604-6668 or FTS 464-6668

16. Abstract

A rigid flap-lag blade analysis has been developed to simulate a rotor in a wind tunnel undergoing an emergency power shutdown. Results show that for a rotor at a nonzero shaft tilt angle undergoing an emergency power shutdown, the oscillatory lag response is divergent. The mean lag response is large when tested at high collective pitch angles. Reducing the collective pitch during the emergency shutdown reduces the steady lag response. Increasing the rotor shaft tilt angle increases the oscillatory lag response component. The blade lag response obtained by incorporating a nonlinear lag damper model indicates that in this case the equivalent linear viscous damping is lower than originally expected. Simulation results indicate that large oscillatory lag motions can be suppressed if the rotor shaft is returned to the fully vertical position during the emergency power shutdown.

17. Key Words (Suggested by Author(s))	18. Distribution Statement
Dynamic analysis Rotor power shutdown Rotor blade response	Unclassified-Unlimited Subject Category - 01

19. Security Classif. (of this report)	20. Security Classif. (of this page)	21. No. of Pages	22. Price
Unclassified	Unclassified	28	A03

For sale by the National Technical Information Service, Springfield, Virginia 22161